

Convection heat transfer coefficients for axial flow gas quenching of a cylinder

Roland Wiberg

FaxénLaboratoriet, Department of Mechanics, Royal Institute of Technology (KTH), 100 44 Stockholm, Sweden

Noam Lior

Dept. of Mechanical Engin. and Appl. Mechanics, University of Pennsylvania, Philadelphia, PA 19104-6315, U.S.A.

Abstract

During gas quenching of steel the local heat transfer rate is of major importance for the final hardness, its uniformity, and the distortion of the parts. The local heat transfer coefficient distributions on a two-diameter long cylinder (150 mm in diameter) was measured in axial flows of air, at Reynolds numbers (Re) of 8.9×10^4 to 6.17×10^5 (9 to 63 m/s). The measurements were performed at different upstream air flow conditions, which were set by varying the flow turbulence level (Tu) using a turbulence generating grid, and by using flow modification inserts in front of the cylinder. The heat transfer coefficients were evaluated from the measured surface temperatures using a thermochromic liquid crystal (TLC) technique. The TLC was applied onto an electrically heated thin foil, which allowed for full surface heat transfer measurements including the cylinder ends. The turbulence-generating grid caused an increase in the heat transfer coefficient up to 22 % and when a flow modification insert was used the nonuniformity was reduced up to 35%. The heat transfer coefficient evaluated as a Nusselt number (Nu) was found to increase with Re , and relations between Nu and Re are presented.

IN QUENCHING, the product hardness, uniformity of mechanical properties, and shape distortion depend on the rate and uniformity of the cooling. Gas quenching requires high gas speeds and pressures (typical values are 10 m/s and 10 bar, but they vary widely depending on the application), i.e. turbulent flows with Reynolds numbers typically between a few hundred thousand to a few million. The flows are thus highly turbulent, with separations and reattachments, which create significant convection heat transfer coefficient nonuniformities over the body surface. These coefficients must be controlled in magnitude and uniformity to obtain optimal quench products.

A cylinder is a classical shape of interest to quenching, but despite a fair number of experimental studies that provide heat transfer coefficient distributions for single cylinders (cf. Lowery 1975 [1], Achenbach 1975 [2], Zukauskas 1985 [3], Wiberg 2000 [4]) and multiple ones (cf. Achenbach 1989 [5]) in cross flows, little information is available for cylinders in axial flow, and none were measured for $Re > 5.5 \times 10^4$. Specifically, heat transfer measurements at constant surface heat flux, were performed by Ota and Kon 1977 [6], for $2.52 \times 10^4 < Re < 5.36 \times 10^4$ and turbulent intensity (Tu) = 0.8%, $L/D=13$ and by Sparrow et al. 1987 [7] for $8 \times 10^3 < Re < 4.7 \times 10^4$ and $Tu = 0.5\%$, $L/D=10$. Kiyama et al. 1991 [8] performed velocity and turbulence measurements of the flow around a circular cylinder in an axial flow, for $Re = 2 \times 10^5$, $Tu < 0.2$, $L/D = 10\%$.

Nomenclature

D : cylinder diameter.

Nu : local Nusselts number, [-]

Re : Reynolds number [-]

Tu : free stream turbulence, [-].

U_∞ : upstream average gas velocity, [m/s].

u : upstream fluctuating gas velocity, [m/s].

q'' : electrically supplied surface heat flux, [W/m^2].

T_s : local surface temperature, [$^\circ C$].

T_∞ : upstream gas temperature, [$^\circ C$].

h : local convection heat transfer coeff., [$W/(m^2 \cdot ^\circ C)$].

ν_∞ : kinematic viscosity of the upstream gas, [m^2/s].

k_∞ : heat conductivity of the upstream gas, [$W/(m \cdot ^\circ C)$].

Nu_{a-b} , Nu_{b-c} , Nu_{c-d} , Nu_{a-d} : averages of Nu .

a, b, c, d : positions along the cylinder (a, d : at the surface center, b, c : at the edges).

x, y : local coordinats in the test section, [mm].

σ_{Nu} : relative standard deviation in Nu , [-].

TLC: Thermochromic Liquid Crystals.

The experimental technique

The present measurements were performed on a cylinder with $L/D = 2.00$ for $8.9 \times 10^4 < Re < 6.17 \times 10^5$, in non affected axial flows, and in axial flows affected from flow modification inserts upstream of the cylinder. A closed loop wind tunnel with a 0.8×1.2 m test section (black inside) and a glass window for visual access, was used for the measurements, see Fig. 1. An opening slit in the roof of the test section maintained the pressure atmospheric. During the measurements the air flow temperature was in the range 25 to 28 °C and the flow velocities from 9 to 64 m/s, while the cylinder surface temperatures were within 36 to 63 °C.

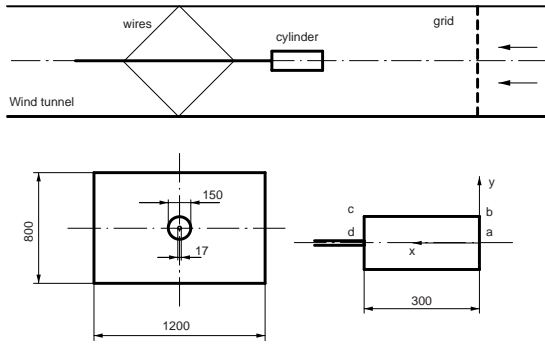


Figure 1: The test section with the cylinder inside.

The measurement of the convection heat transfer coefficient distribution on the cylinder surfaces, was made by electrically applying a constant heat flux to a thin foil applied to the cylinder surface, and measuring the surface temperature distribution on the foil by using thermochromic liquid crystals (TLC) coated on the foil. These crystals change their color with temperature, and digital video photographs of the TLC were translated to temperatures by image processing software developed by us for this purpose, associated with a careful calibration.

The heat transfer coefficient. A Sony DCR-TRV 900E camera, 680×510 pixels, 24 bit color resolution and two 24°, 50 W halogen lamps fixed to the camera, were used for the photographs. The local surface temperatures T_s were evaluated from the colors, and the convection heat transfer coefficient h was calculated using equation eq. 1, where the electrically supplied heat flux q'' , was reduced by a calculated radiation loss, (typically 5 -10 % of q'') and where T_∞ was the upstream air temperature.

$$q'' - 5.67 \times 10^{-8} (T_s^4 - T_\infty^4) = h(T_s - T_\infty) \quad (1)$$

The test cylinder. The test cylinder had the diameter $D = 150$ mm and the length $L = 300$ mm and made of solid extruded polystyrene (EPS), ($k = 0.033 \text{ W}/(m^\circ\text{C})$). Four thermocouples were mounted just under the EPS surface, on which a $125 \mu\text{m}$ plastic film was glued to make the surface smooth. A foil made of strips of the metal Inconel ($12 \mu\text{m}$

thick, $k = 12 \text{ W}/(m^\circ\text{C})$), was glued on the film all over the surface including the two cylinder ends, except within $0.01 D$ (1.5 mm) from the cylinder edges. The foil resistance measured over 42 sub-surfaces was found within $\pm 1.5\%$. Manually variable transformers (A.C.) were used to provide the foil with a constant power, which was found to vary within $\pm 1.5\%$. The heat conduction loss in the cylinder was calculated within 2%, larger near the cylinder edges, where the data therefore was canceled.

The whole foil was spray coated with black backing paint, and then with TLC R35C20 C17-10 (supplied by Hallcrest in UK) in a band along the cylinder. To assist the detection of flow direction, thin and soft cotton tufts were taped on the surface in a row along the cylinder, 10 mm apart. A steel pipe $0.113 D$ (17 mm) in diameter was glued into the cylinder for its support in the wind tunnel, and the pipe was held by eight 2 mm thick steel wires, which centered and aligned the cylinder, to the test section walls. Vibrations appeared on the cylinder, which were estimated by visual means to ± 0.5 mm.

The used configurations. The measurements were performed in four different configurations: A) the cylinder alone in a low upstream turbulence flow, $Tu = 0.3\%$ B) the cylinder in an upstream flow affected by turbulence-generating grid, $Tu = 6.7\%$ C) the cylinder placed downstream of a circular disc $1/3 D$ (50 mm) in diameter, which was centered on the cylinder axis and located at $x = -1.00 D$ ($x = -150$ mm), D) the cylinder placed downstream of a circular disc $2/3 D$ (100 mm) in diameter, at the same position. These discs were $0.0333 D$ (5 mm) thick with sharp corners and fixed using 0.5 mm wires to the test section walls.

The turbulence generating grid was located upstream of the cylinder at $x = -5.50 D$ ($x = -825$ mm) and made of square rods 10×10 mm, 50 mm apart. The turbulence level was measured using a hot wire anemometer with a single hot wire $2.5 \mu\text{m}$ in diameter, at the average flow velocity 18 m/s and without the cylinder at $x = 0.00$. The turbulence level is defined, in Eq. 2, where U_∞ is the average velocity in the x -direction and u the fluctuating velocity in the same direction.

$$Tu = \frac{\sqrt{u^2}}{U_\infty} \quad (2)$$

Calibration of the TLC. The TLC was calibrated before and after the measurements in-situ on the cylinder inside the test section, using the thermocouples in the surface as reference. Color photographs of the TLC on the cylinder were taken through the glass window from fixed positions. Hue was calculated using the function (rgb2hsv) in Matlab 5.2.1 and related to the temperature.

The uniformity in hue read from the TLC, was tested in an isothermal room and in the most sensitive part of the TLC range. Using the same camera settings, view angle and light source as during the calibration. A local correction was then performed by interpolating between the found in-situ calibration curves in proportion to hue found in the isothermal test. The errors in the local TLC measured temperatures ($T_s - T_\infty$), were then estimated within $\pm 5\%$.

Measure procedure. The wind tunnel was started, the upstream flow velocity U_∞ measured using a Prandtl tube, and the flow temperature T_∞ , were allowed to stabilize. The electrical power generating the surface heat flux q'' of the foil was increased until the surface temperatures came within the active temperature interval of the TLC, and the temperatures were then allowed to stabilize, typically over 5-10 minutes. In the steady state, color photographs of the TLC were captured after which the electrical heat to the foil was shut off. This procedure was repeated for each measurement. The temperature data was then smoothed by averaging within $\pm 0.0267 D$ along the surface a-d.

The Nusselt numbers. The convection heat transfer coefficient h was expressed in terms of the Nusselt number Nu (dimensionless), as can be seen in Eq. 3, where k_∞ is the heat conductivity of the upstream air. The averages of Nu were calculated as a weighted surface averages, surface-weighted averages were calculated for the front end surface a-b, see Fig. 1, for the middle surface b-c, for the rear end surface c-d and for the whole surface a-d. The averages were evaluated, using the assumption that the heat transfer distribution was symmetric around the cylinder axis. A non-uniformity number, was calculated as a surface weighted relative standard deviation in Nu along the surface a-d, σ_{Nu} .

$$Nu = \frac{hD}{k_\infty} \quad (3)$$

The Reynolds number dependence. The Reynolds number for the flow around the cylinder, is defined in Eq. 4, in where ν_∞ was the kinematic viscosity of the upstream air. Nu was assumed proportional to Re , when raised to the exponent e , as can be seen in Eq. 5, where C and e were unknown constants. Nu was measured at three different Re , giving three pairs of Nu and Re for every position along the surface, the constants were found by searching the value of e , which minimized the relative differences in C .

$$Re = \frac{U_\infty D}{\nu_\infty} \quad (4)$$

$$Nu = C \times Re^e \quad (5)$$

Error estimates. Based on error analysis, the error in the local Nu was estimated to be $\pm 6\%$, and in $Re \pm 2\%$. The relation seen in Eq. 5 with the found constants, could predict the measured local and averaged Nu within 3%.

Experimental results

Heat transfer in configuration (A). Measurements of the heat transfer coefficient distribution on the cylinder were performed, at low upstream turbulence levels ($Tu = 0.3\%$), and at Reynolds numbers (Re) of 6.17×10^5 , 3.22×10^5 and 1.77×10^5 . The Nusselt number distribution along the cylinder surface is shown in Fig. 2. Nu is seen to increase with Re , as expected, and the characteristic shape of the curves is similar for all Re .

On the front (upstream) surface of the cylinder perpendicular to the flow direction, a-b, Nu increases towards the edge. The average Nu is significantly higher along the surface b-c, increasing from the front edge by at least two-fold to a maximal value at a distance of $1.50 D$ from the front edge. The interval in which a shift in the average flow direction (flow reattachment) appeared, was detected using the tufts on the surface at $Re = 1.75 \times 10^5$, and was found to be at $1.465 - 1.535 D$ from the front edge, which agreed with the position found for the maximal Nu .

The position of reattachment was also found to be similar to results by Kiya et al. 1991 [8]. An extrapolation of the maximal Nu at this position was performed, using the found exponent to a lower Re level gave Nu similar to that measured by Sparrow et al. 1987 [7].

On the rear surface c-d, Nu drops to about half the previous values, increasing from the edge. The average Nusselt number along the surface a-d, was for these three Reynolds numbers found to be $Nu_{a-d} = 1020, 658$ and 433 , respectively.

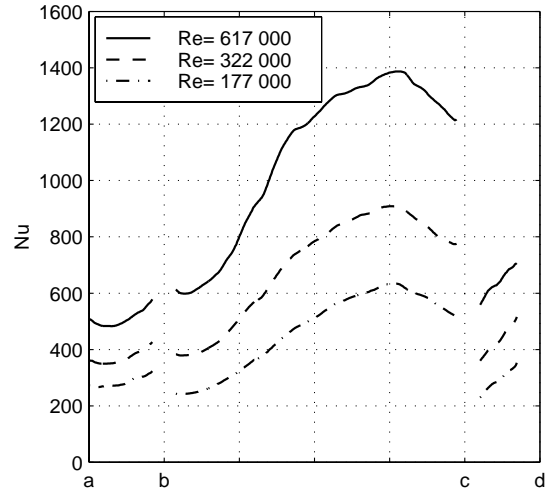


Figure 2: Nusselt numbers along the cylinder surface, from the measurements in configuration (A).

Heat transfer in configuration (B). A turbulence generating grid was inserted upstream of the cylinder, generating free stream turbulence intensity, Tu of 6.7% , and at Reynolds numbers of 3.23×10^5 , 1.77×10^5 and 8.9×10^4 . The Nusselt number distribution along the cylinder surface is shown in Fig. 3. Nu is seen to increase with Re , as expected, and the characteristic shape of the curves is similar for all Re .

On the front (upstream) surface of the cylinder, a-b, the heat transfer profiles are almost flat. The average of Nu is significantly higher along the surface b-c, on where a maximum was found at $0.90 D$ from the front edge. The reattachment of the flow, measured at $Re = 1.75 \times 10^5$ using tufts, was found to be within $1.00 - 1.13 D$ from the front edge. On the rear surface c-d, Nu drops to a lower value, increasing from the edge. The average along the whole surface a-d, was for these

three Reynolds numbers found to be $Nu_{a-d} = 803, 535$ and 337 , respectively.

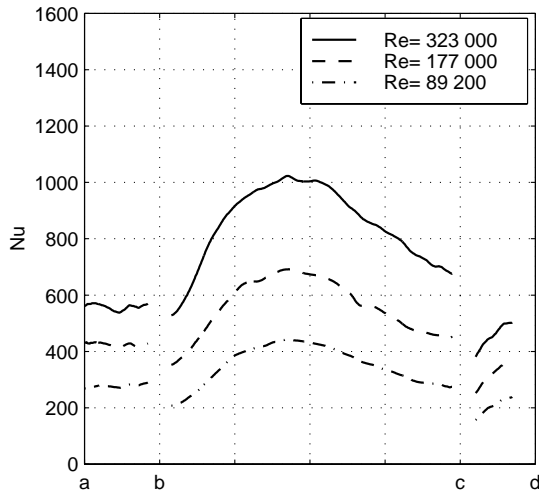


Figure 3: Nusselt numbers along the cylinder surface, from the measurements in axial flows with upstream turbulence $Tu = 6.7\%$, configuration (B).

Heat transfer in configuration (C). A disk with diameter $1/3 D$ was placed upstream of the cylinder as detailed earlier, and at Reynolds numbers of $Re = 6.09 \times 10^5$, 3.23×10^5 and 1.77×10^5 . The Nusselt number distribution along the cylinder surface is shown in Fig. 4. Nu is seen to increase with Re , as expected, and the characteristic shape of the curves is similar for all Re .

On the front (upstream) surface of the cylinder, a-b, Nu increases from the center to the corner. On the surface b-c, a maximal value in Nu appear close to front edge and a decrease is seen towards the rear edge, reaching a halved level. On the rear surface c-d, Nu was lower, increasing from the corner. The average Nusselt number along the surface a-d, was for these three Re found to be $Nu_{a-d} = 1190, 777$ and 481 , respectively.

A test was performed with the disc closer to the cylinder, located $0.50 D$ from front surface. The heat transfer on the front surface a-b, was then found to be asymmetric, when the distance was increased to $1.00 D$, the heat transfer was again symmetric. This indicated that the flow was sensitive to disturbances when the disc was closer to the cylinder.

Heat transfer in configuration (D). Here a disc with the diameter $2/3 D$ was placed upstream of the cylinder as detailed earlier, and the Reynolds numbers was $Re = 6.14 \times 10^5$. The Nusselt number distribution along the cylinder surface is shown in Fig. 5. On the front (upstream) surface of the cylinder, a-b, Nu increases from the center to the corner. On the surface b-c, the levels are similar as on the front surface a-b, and a maximal level is seen at the front edge, from which a decrease is seen towards the rear edge. On the rear surface c-d, Nu was even lower, increasing from the corner. The average Nusselt number along the surface a-d, was found to be

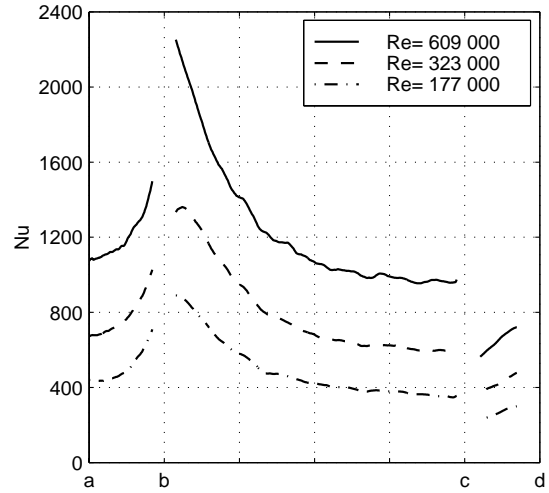


Figure 4: Nusselt numbers along the cylinder surface, from the measurements in flows with a $1/3 D$ diameter disk placed $1.00 D$ upstream of the cylinder, configuration (C).

$$Nu_{a-d} = 1080.$$

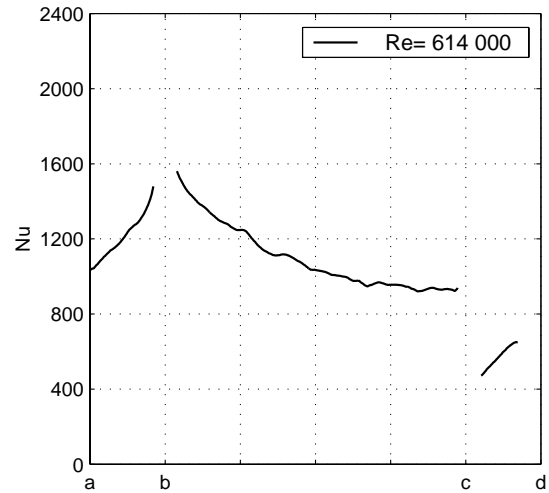


Figure 5: Nusselt numbers along the cylinder surface, measurements using a $2/3 D$ diameter disk placed $1.00 D$ upstream of the cylinder, configuration (D).

The Reynolds number dependence. The assumed relation between Nu and the Re seen in eq. 5, was fitted to the measured averages of Nu for each of the surfaces (a-b, b-c, c-d, and the whole cylinder a-d) and for the three configurations (A), (B), (C), and the found constants in the relation are given in Table 1.

The observed similarity of the curves which describe the dependence of Nu on Re for all Reynolds numbers investigated here indicates that it may be possible to find a value of the power ϵ that would describe the behavior of the local Nu with respect to Re . These values, for all cylinder surfaces for the configurations (A), (B) and (C), were calculated and are

Table 1: The constants C and e of eq. 5 for the averages of Nu on the surfaces (a-b, b-c, c-d, and a-d).

Config.	Const.	a-b	b-c	c-d	a-d
(A)	C	1.070	0.126	0.122	0.138
	e	0.464	0.680	0.642	0.668
(B)	C	0.615	0.141	0.156	0.155
	e	0.538	0.686	0.628	0.674
(C)	C	0.155	0.058	0.055	0.068
	e	0.676	0.748	0.704	0.734

shown in Fig 6. There are obvious local errors in e caused by the local errors in the measured Nu , anyway, some conclusions may be drawn.

On the front surface a-b, and for configurations (A) and (B) it was found that e increased with an increase in Tu , while e was even larger when measured using the disc in configuration (C). The magnitudes of the averages of e on surface a-b, can be seen in Table 1.

On the middle surface b-c, e had a minimal value, where Nu had a maximal value; e had a minimum for configuration (A) at $1.50 D$ from the front edge, for configuration (B) at $0.75-0.96 D$ from the front edge, and for configuration (C) at $0.275 D$ from the front edge. For all the configurations, e was found to increase in a similar way, from the minimum and towards the rear. On the rear surface c-d, for each of the configurations, e was found somewhat lower than on the middle surface b-c, decreasing from the edge.

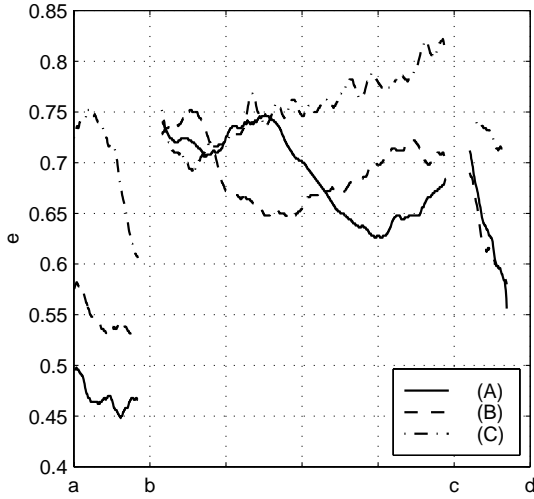


Figure 6: The found local exponents e of eq. 5, for the configurations (A), (B) and (C).

Discussion

The variations in Nu was relatively small over the front surface a-b, for both the configurations (A) and (B). The increase in Tu from 0.3 to 6.7 %, at a constant Re , caused

Table 2: Average heat transfer coefficients and their nonuniformities for a typical gas quenching case, nitrogen quenchant at 10 bar, 300 K and a flow velocity of 20 m/s against a cylinder 49 mm in diameter.

config.	Nu_m	$h_m W/(mK)$	σ_{Nu}
(A)	1020	558	0.31
(B)	1240	679	0.22
(C)	1200	663	0.30
(D)	1080	594	0.20

an increase in Nu_{a-b} of 46 %, which is similar to the results, found on the front of a circular cylinder in cross flow, by Lowery et al. 1975 [1].

On the middle surface b-c, the position of the maximal Nu was found to move towards the front when Tu was increased, configuration (A) and (B). At the same time the position of the flow reattachment moved towards the front, but to a lesser extent. The discs used in the configurations (C) and (D) are assumed generating an increased turbulence towards the cylinder, and furthermore some confinements of the upstream flow. The position of maximum Nu moved for these configurations closer to the front edge.

On the rear surface c-d, Nu was fairly similar for all the configurations (A), (B), (C), (D) and for a fixed Re , which indicated a low sensitivity to the different upstream flow conditions.

An example of a gas cooling. As stated in the introduction, quenching is improved with the magnitude and uniformity of the cooling heat transfer coefficients. A comparison between the configurations (A), (B), (C) and (D) was performed, for a representative example: nitrogen quenchant at 10 bar, 300 K and a flow velocity of 20 m/s. A cylinder of 49 mm diameter will give a Reynolds number for this flow of $Re = 6.14 \times 10^5$.

The averages Nu_{a-d} were calculated using eq. 5, using the coefficients C and e found in this study. The convection heat transfer coefficient h_{a-d} was then evaluated from eq. 3 and the results are presented in table 2. The coefficient h_{a-d} was in configuration (B) found to be 22 %, in (C) 19 % and in (D) 6 % higher than in configuration (A).

The non-uniformity in Nu (and h) σ_{Nu} was found lower compared to configuration (A) by 29 % in configuration (B) and by 35% in configuration (D), while for configuration (C) the reduction was found small. Configuration (B) generated the highest heat transfer and also at a low non-uniformity, and may therefore be the best choice. However, the upstream grid may generate an undesirable pressure drop, a possible solution to this problem could be to use a grid locally in front of the cylinder, or another smaller disturbance of the flow, which can generate a similar result at a lower pressure drop.

Conclusions

The local heat transfer coefficient distributions on a two-

diameter long cylinder (150 mm in diameter) was measured in axial flows of air, at Reynolds numbers (Re) of 8.9×10^4 to 6.17×10^5 (9 to 63 m/s). The measurements were performed inside a closed loop wind tunnel at different upstream flow conditions, which were set by varying the flow turbulence level (Tu) using a turbulence generating grid, and by using flow modification inserts in front of the cylinder. The flow modification inserts were found to create a major change in the local heat transfer coefficient distribution and reduced its nonuniformity, and the measured position of flow reattachment on the cylinder surface using tufts, gave insight to the found maximum in the local heat transfer coefficient.

The turbulence generating grid caused an increase in the heat transfer coefficient up to 22 % and when a flow modification insert was used the nonuniformity was reduced up to 35%. The heat transfer coefficient evaluated as a Nusselt number (Nu) was found to increase with the Reynolds number (Re) of the flow, but at different amounts for different locations on the cylinder, and relations between the Nu and Re were evaluated and presented.

Acknowledgment

This work was partially supported by AGA AB (now Linde Gas) and Ipsen International GmbH.

References

- [1] Lowery and R.I. Vachon, The effect of turbulence on heat transfer from heated cylinders, *Journal of Heat and Mass Transfer*, 1975, vol. 18, pp. 1229- 1242.
- [2] Achenbach E., Total and local heat transfer from a smooth circular cylinder in cross-flow at high Reynolds number, *Int. J. Heat Mass transfer*, 1975, Vol. 18, pp. 1387-1396.
- [3] Zukauskas, J. Ziugzda, *Heat Transfer of a cylinder in Crossflow*, Springer- Verlag: Berlin, 1985.
- [4] Wiberg Roland, Muhammad-Klingmann Barbro, Ferrari Jerome and Lior Noam, Use of Thermochromic Coatings for the Experimental Determination of the Distribution of Heat Transfer Coefficients in Gas-Cooled Quenching, 5th ASM Heat Treatment and Surface Engineering Conference in Europe, Gothenburg, Sweden 7 - 9 June 2000.
- [5] Achenbach E., Heat transfer from a staggered tube bundle in cross-flow at high Reynolds numbers, *Int. J. Heat Mass transfer*, 1989, Vol. 32, No. 2, pp. 271-280.
- [6] Terukazu Ota, Nobuhiko Kon, Heat transfer in an axisymmetric separated and reattached flow over a longitudinal blunt circular cylinder, *Journal of Heat Transfer*, February 1977, pp. 155- 157.
- [7] Sparrow EM, Kang SS, Chuck W, Relation between the points of flow reattachment and maximum heat-transfer for regions of flow separation, *International journal of heat and mass transfer*, 1987, 30 (7): 1237-1246.
- [8] Kiya, M. (Hokkaido Univ., Sapporo, Japan) ; Mochizuki, O.; Tamura, H.; Nozawa, T.; Ishikawa, R.; Kushioka, K., Turbulence properties of an axisymmetric separation-and-reattaching flow, *AIAA Journal*, June 1991, v 29, n 6, p 936-41.